

¹ **Power laws and critical transitions in global forests**

² **Leonardo A. Saravia^{1 3}, Santiago R. Doyle¹, Ben Bond-Lamberty²**

³ 1. Instituto de Ciencias, Universidad Nacional de General Sarmiento, J.M. Gutierrez 1159 (1613), Los
⁴ Polvorines, Buenos Aires, Argentina.

⁵ 2. Pacific Northwest National Laboratory, Joint Global Change Research Institute at the University of
⁶ Maryland–College Park, 5825 University Research Court #3500, College Park, MD 20740, USA

⁷ 3. Corresponding author e-mail: lsaravia@ungs.edu.ar

⁸ **Keywords:** Forest fragmentation, early warning signals, percolation, power-laws, MODIS, critical transitions

⁹ **Running title:** Critical fragmentation in global forest

¹⁰ **Abstract**

¹¹ Forests provide critical habitat for many species, essential ecosystem services, and are coupled to atmospheric
¹² dynamics through exchanges of energy, water and gases. One of the most important changes produced in
¹³ the biosphere is the replacement of forest areas with human dominated landscapes. This usually leads to
¹⁴ fragmentation, altering the sizes of patches, the structure and function of the forest. Here we studied the
¹⁵ distribution and dynamics of forest patch sizes at a global level, examining signals of a critical transition
¹⁶ from an unfragmented to a fragmented state. We used MODIS vegetation continuous field to estimate the
¹⁷ forest patches at a global level and defined wide regions of connected forest across continents and big islands.
¹⁸ We search for critical phase transitions, where the system state of the forest changes suddenly at a critical
¹⁹ point in time; this implies an abrupt change in connectivity that causes an increased fragmentation level.
²⁰ We combined five criteria to evaluate the closeness of the system to a fragmentation threshold, studying in
²¹ particular the distribution of forest patch sizes and the dynamics of the largest patch over the last sixteen
²² years. We found that forest fragments of all continental regions followed a power-law distribution over
²³ the fifteen years. We also found that the Philippines region probably went through a critical transition
²⁴ from a fragmented to an unfragmented state. Regions with the highest deforestation rates—South America,
²⁵ Southeast Asia, Africa—all met the criteria to be near a critical fragmentation threshold. This implies that
²⁶ human pressures and climate forcings might trigger undesired effects of fragmentation, such as species loss
²⁷ and degradation of ecosystems services, in these regions. The simple criteria proposed here could be used as
²⁸ an early warning to estimate the distance to a fragmentation threshold in forests around the globe.

²⁹ **Introduction**

³⁰ Forests are one of the most important biomes on earth, providing habitat for a large proportion of species
³¹ and contributing extensively to global biodiversity (Crowther *et al.* 2015). In the previous century human
³² activities have influenced global bio-geochemical cycles (Bonan 2008; Canfield *et al.* 2010), with one of
³³ the most dramatic changes being the replacement of 40% of Earth's formerly biodiverse land areas with
³⁴ landscapes that contain only a few species of crop plants, domestic animals and humans (Foley *et al.* 2011).

³⁵ These local changes have accumulated over time and now constitute a global forcing (Barnosky *et al.* 2012).
³⁶ Another global scale forcing that is tied to habitat destruction is fragmentation, which is defined as the
³⁷ division of a continuous habitat into separated portions that are smaller and more isolated. Fragmentation
³⁸ produces multiple interwoven effects: reductions of biodiversity between 13% and 75%, decreasing forest
³⁹ biomass, and changes in nutrient cycling (Haddad *et al.* 2015). The effects of fragmentation are not only
⁴⁰ important from an ecological point of view but also that of human activities, as ecosystem services are deeply
⁴¹ influenced by the level of landscape fragmentation (Rudel *et al.* 2005; Angelsen 2010; Mitchell *et al.* 2015).

⁴² Ecosystems have complex interactions between species and present feedbacks at different levels of organi-
⁴³ zation (Gilman *et al.* 2010), and external forcings can produce abrupt changes from one state to another,
⁴⁴ called critical transitions (Scheffer *et al.* 2009). Such 'critical' transitions have been detected mostly at local
⁴⁵ scales (Drake & Griffen 2010; Carpenter *et al.* 2011), but the accumulation of changes in local communities
⁴⁶ that overlap geographically can propagate and theoretically cause an abrupt change of the entire system at
⁴⁷ larger scales (Barnosky *et al.* 2012).

⁴⁸ Complex systems can experience two general classes of critical transitions (Solé 2011). In so-called first
⁴⁹ order transitions, a catastrophic regime shift that is mostly irreversible occurs because of the existence of
⁵⁰ alternative stable states (Scheffer *et al.* 2001). This class of transitions is suspected to be present in a variety
⁵¹ of ecosystems such as lakes, woodlands, coral reefs (Scheffer *et al.* 2001), semi-arid grasslands (Bestelmeyer
⁵² *et al.* 2011), and fish populations (Vasilakopoulos & Marshall 2015). They can be the result of positive
⁵³ feedback mechanisms (Villa Martín *et al.* 2015); for example, fires in some forest ecosystems were more
⁵⁴ likely to occur in previously burned areas than in unburned places (Kitzberger *et al.* 2012).

⁵⁵ The other class of critical transitions are continuous or second order transitions (Solé & Bascompte 2006). In
⁵⁶ these cases, there is a narrow region where the system suddenly changes from one domain to another, with
⁵⁷ the change being continuous and in theory reversible. This kind of transitions were suggested to be present
⁵⁸ in tropical forests (Pueyo *et al.* 2010; Taubert *et al.* 2018), semi-arid mountain ecosystems (McKenzie
⁵⁹ & Kennedy 2012), and tundra shrublands (Naito & Cairns 2015). The transition happens at a critical

60 point where we can observe a distinctive spatial pattern: scale invariant fractal structures characterized by
61 power law patch distributions (Stauffer & Aharony 1994). There are several processes that can convert a
62 catastrophic transition to a second order transitions (Villa Martín *et al.* 2015). These include stochasticity,
63 such as demographic fluctuations, spatial heterogeneities, and/or dispersal limitation. All these components
64 are present in forest around the globe (Seidler & Plotkin 2006; Filotas *et al.* 2014; Fung *et al.* 2016),
65 and thus continuous transitions might be more probable than catastrophic transitions. Moreover there is
66 some evidence of recovery in some systems that supposedly suffered an irreversible transition produced by
67 overgrazing (Zhang *et al.* 2005; Bestelmeyer *et al.* 2013) and desertification (Allington & Valone 2010).

68 The spatial phenomena observed in continuous critical transitions deal with connectivity, a fundamental
69 property of general systems and ecosystems from forests (Ochoa-Quintero *et al.* 2015) to marine ecosystems
70 (Leibold & Norberg 2004) and the whole biosphere (Lenton & Williams 2013). When a system goes from a
71 fragmented to a connected state we say that it percolates (Solé 2011). Percolation implies that there is a
72 path of connections that involves the whole system. Thus we can characterize two domains or phases: one
73 dominated by short-range interactions where information cannot spread, and another in which long range
74 interactions are possible and information can spread over the whole area. (The term “information” is used
75 in a broad sense and can represent species dispersal or movement.) Thus, there is a critical “percolation
76 threshold” between the two phases, and the system could be driven close to or beyond this point by an
77 external force; climate change and deforestation are the main forces that could be the drivers of such a phase
78 change in contemporary forests (Bonan 2008; Haddad *et al.* 2015). There are several applications of this
79 concept in ecology: species’ dispersal strategies are influenced by percolation thresholds in three-dimensional
80 forest structure (Solé *et al.* 2005), and it has been shown that species distributions also have percolation
81 thresholds (He & Hubbell 2003). This implies that pushing the system below the percolation threshold could
82 produce a biodiversity collapse (Bascompte & Solé 1996; Solé *et al.* 2004; Pardini *et al.* 2010); conversely,
83 being in a connected state (above the threshold) could accelerate the invasion of forest into prairie (Loehle
84 *et al.* 1996; Naito & Cairns 2015).

85 One of the main challenges with systems that can experience critical transitions—of any kind—is that the
86 value of the critical threshold is not known in advance. In addition, because near the critical point a small
87 change can precipitate a state shift of the system, they are difficult to predict. Several methods have been
88 developed to detect if a system is close to the critical point, e.g. a deceleration in recovery from perturbations,
89 or an increase in variance in the spatial or temporal pattern (Hastings & Wysham 2010; Carpenter *et al.*
90 2011; Boettiger & Hastings 2012; Dai *et al.* 2012).

91 The existence of a critical transition between two states has been established for forest at a global scale in

92 different works (Hirota *et al.* (2011); Staal *et al.* (2016); Wuyts *et al.* (2017)). It is generally believed that
93 this constitutes a first order catastrophic transition. The regions where forest can grow are not distributed
94 homogeneously, as there are demographic fluctuations in forest growth and disturbances produced by human
95 activities. All these factors imply that if these were first order transitions they will be converted or observed
96 as second order continuous transitions (Villa Martín *et al.* 2014, 2015). From this basis, we applied indices
97 derived from second order transitions to global forest cover dynamics.

98 In this study, our objective is to look for evidence that forests around the globe are near continuous critical
99 points that represent a fragmentation threshold. We use the framework of percolation to first evaluate if
100 forest patch distribution at a continental scale is described by a power law distribution and then examine
101 the fluctuations of the largest patch. The advantage of using data at a continental scale is that for very large
102 systems the transitions are very sharp (Solé 2011) and thus much easier to detect than at smaller scales,
103 where noise can mask the signals of the transition.

104 Methods

105 Study areas definition

106 We analyzed mainland forests at a continental scale, covering the whole globe, by delimiting land areas with
107 a near-contiguous forest cover, separated with each other by large non-forested areas. Using this criterion,
108 we delimited the following forest regions. In America, three regions were defined: South America temperate
109 forest (SAT), subtropical and tropical forest up to Mexico (SAST), and USA and Canada forest (NA). Europe
110 and North Asia were treated as one region (EUAS). The rest of the delimited regions were South-east Asia
111 (SEAS), Africa (AF), and Australia (OC). We also included in the analysis islands larger than 10^5km^2 . The
112 mainland region has the number 1 e.g. OC1, and the nearby islands have consecutive numeration (Appendix
113 S4, figure S1-S6). We applied this criterion to delimit regions because we based our study on percolation
114 theory that assumes some kind of connectivity in the study area.

115 Forest patch distribution

116 We studied forest patch distribution in each defined area from 2000 to 2015 using the MODerate-resolution
117 Imaging Spectroradiometer (MODIS) Vegetation Continuous Fields (VCF) Tree Cover dataset version 051
118 (DiMiceli *et al.* 2015). This dataset is produced at a global level with a 231-m resolution, from 2000 onwards
119 on an annual basis, the last available year was 2015. There are several definition of forest based on percent

120 tree cover (Sexton *et al.* 2015); we choose a range from 20% to 40% threshold in 5% increments to convert
121 the percentage tree cover to a binary image of forest and non-forest pixels. This range is centered in the
122 definition used by the United Nations' International Geosphere-Biosphere Programme (Belward 1996), and
123 studies of global fragmentation (Haddad *et al.* 2015) and includes the range used in other studies of critical
124 transitions (Xu *et al.* 2016). Using this range we try to avoid the errors produced by low discrimination
125 of MODIS VCF between forest and dense herbaceous vegetation at low forest cover and the saturation of
126 MODIS VCF in dense forests (Sexton *et al.* 2013). We repeat all the analysis for this set of thresholds,
127 except in some specific cases described below. Patches of contiguous forest were determined in the binary
128 image by grouping connected forest pixels using a neighborhood of 8 forest units (Moore neighborhood).
129 The MODIS VCF product defines the percentage of tree cover by pixel, but does not discriminate the type
130 of trees so besides natural forest it includes plantations of tree crops like rubber, oil palm, eucalyptus and
131 other managed stands (Hansen *et al.* 2014).

132 **Percolation theory**

133 A more in-depth introduction to percolation theory can be found elsewhere (Stauffer & Aharony 1994) and a
134 review from an ecological point of view is available (Oborny *et al.* 2007). Here, to explain the basic elements
135 of percolation theory we formulate a simple model: we represent our area of interest by a square lattice
136 and each site of the lattice can be occupied—e.g. by forest—with a probability p . The lattice will be more
137 occupied when p is greater, but the sites are randomly distributed. We are interested in the connection
138 between sites, so we define a neighborhood as the eight adjacent sites surrounding any particular site. The
139 sites that are neighbors of other occupied sites define a patch. When there is a patch that connects the
140 lattice from opposite sides, it is said that the system percolates. When p is increased from low values, a
141 percolating patch suddenly appears at some value of p called the critical point p_c .

142 Thus percolation is characterized by two well defined phases: the unconnected phase when $p < p_c$ (called
143 subcritical in physics), in which species cannot travel far inside the forest, as it is fragmented; in a general
144 sense, information cannot spread. The second is the connected phase when $p > p_c$ (supercritical), species
145 can move inside a forest patch from side to side of the area (lattice), i.e. information can spread over the
146 whole area. Near the critical point several scaling laws arise: the structure of the patch that spans the area
147 is fractal, the size distribution of the patches is power-law, and other quantities also follow power-law scaling
148 (Stauffer & Aharony 1994).

149 The value of the critical point p_c depends on the geometry of the lattice and on the definition of the

150 neighborhood, but other power-law exponents only depend on the lattice dimension. Close to the critical
151 point, the distribution of patch sizes is:

152 (1) $n_s(p_c) \propto s^{-\alpha}$

153 where $n_s(p)$ is the number of patches of size s . The exponent α does not depend on the details of the
154 model and it is called universal (Stauffer & Aharony 1994). These scaling laws can be applied for landscape
155 structures that are approximately random, or at least only correlated over short distances (Gastner *et al.*
156 2009). In physics this is called “isotropic percolation universality class”, and corresponds to an exponent
157 $\alpha = 2.05495$. If we observe that the patch size distribution has another exponent it will not belong to this
158 universality class and some other mechanism should be invoked to explain it. Percolation thresholds can also
159 be generated by models that have some kind of memory (Hinrichsen 2000; Ódor 2004): for example, a patch
160 that has been exploited for many years will recover differently than a recently deforested forest patch. In
161 this case, the system could belong to a different universality class, or in some cases there is no universality,
162 in which case the value of α will depend on the parameters and details of the model (Corrado *et al.* 2014).

163 To illustrate these concepts, we conducted simulations with a simple forest model with only two states: forest
164 and non-forest. This type of model is called a “contact process” and was introduced for epidemics (Harris
165 1974), but has many applications in ecology (Solé & Bascompte 2006; Gastner *et al.* 2009). A site with forest
166 can become extinct with probability e , and produce another forest site in a neighborhood with probability
167 c . We use a neighborhood defined by an isotropic power law probability distribution. We defined a single
168 control parameter as $\lambda = c/e$ and ran simulations for the subcritical fragmentation state $\lambda < \lambda_c$, with $\lambda = 2$,
169 near the critical point for $\lambda = 2.5$, and for the supercritical state with $\lambda = 5$ (see supplementary data, gif
170 animations).

171 Patch size distributions

172 We fitted the empirical distribution of forest patches calculated for each of the thresholds on the range we
173 previously mentioned. We used maximum likelihood (Goldstein *et al.* 2004; Clauset *et al.* 2009) to fit four
174 distributions: power-law, power-law with exponential cut-off, log-normal, and exponential. We assumed
175 that the patch size distribution is a continuous variable that was discretized by the remote sensing data
176 acquisition procedure.

177 We set a minimal patch size (X_{min}) at nine pixels to fit the patch size distributions to avoid artifacts at patch
178 edges due to discretization (Weerman *et al.* 2012). Besides this hard X_{min} limit we set due to discretization,
179 the power-law distribution needs a lower bound for its scaling behavior. This lower bound is also estimated

180 from the data by maximizing the Kolmogorov-Smirnov (KS) statistic, computed by comparing the empirical
181 and fitted cumulative distribution functions (Clauset *et al.* 2009). For the log-normal model we constrain
182 the values of the μ parameter to positive values, this parameter controls the mode of the distribution and
183 when is negative most of the probability density of the distribution lies outside the range of the forest patch
184 size data (Limpert *et al.* 2001).

185 To select the best model we calculated corrected Akaike Information Criteria (AIC_c) and Akaike weights
186 for each model (Burnham & Anderson 2002). Akaike weights (w_i) are the weight of evidence in favor of
187 model i being the actual best model given that one of the N models must be the best model for that set of
188 N models. Additionally, we computed a likelihood ratio test (Vuong 1989; Clauset *et al.* 2009) of the power
189 law model against the other distributions. We calculated bootstrapped 95% confidence intervals (Crawley
190 2012) for the parameters of the best model, using the bias-corrected and accelerated (BCa) bootstrap (Efron
191 & Tibshirani 1994) with 10000 replications.

192 **Largest patch dynamics**

193 The largest patch is the one that connects the highest number of sites in the area. This has been used
194 extensively to indicate fragmentation (Gardner & Urban 2007; Ochoa-Quintero *et al.* 2015) and the size of
195 the largest patch S_{max} has been studied in relation to percolation phenomena (Stauffer & Aharony 1994;
196 Bazant 2000; Botet & Ploszajczak 2004), but is seldom used in ecological studies (for an exception see
197 Gastner *et al.* (2009)). When the system is in a connected state ($p > p_c$) the landscape is almost insensitive
198 to the loss of a small fraction of forest, but close to the critical point a minor loss can have important effects
199 (Solé & Bascompte 2006; Oborny *et al.* 2007), because at this point the largest patch will have a filamentary
200 structure, i.e. extended forest areas will be connected by thin threads. Small losses can thus produce large
201 fluctuations.

202 One way to evaluate the fragmentation of the forest is to calculate the proportion of the largest patch against
203 the total area (Keitt *et al.* 1997). The total area of the regions we are considering (Appendix S4, figures
204 S1-S6) may not be the same as the total area that the forest could potentially occupy, and thus a more
205 accurate way to evaluate the weight of S_{max} is to use the total forest area, which can be easily calculated
206 by summing all the forest pixels. We calculate the proportion of the largest patch for each year, dividing
207 S_{max} by the total forest area of the same year: $RS_{max} = S_{max} / \sum_i S_i$. This has the effect of reducing the
208 S_{max} fluctuations produced due to environmental or climatic changes influences in total forest area. When
209 the proportion RS_{max} is large (more than 60%) the largest patch contains most of the forest so there are

210 fewer small forest patches and the system is probably in a connected phase. Conversely, when it is low (less
211 than 20%), the system is probably in a fragmented phase (Saravia & Momo 2017). To define if a region will
212 be in a connected or unconnected state we used the RS_{max} of the highest (i.e., most conservative) threshold
213 of 40%, that represent the most dense area of forest within our chosen range. We assume that there are
214 two alternative states for the critical transition—the forest could be fragmented or unfragmented. If RS_{max}
215 is a good indicator of the fragmentation state of the forest its distribution of frequencies should be bimodal
216 (Bestelmeyer *et al.* 2011), so we apply the Hartigan’s dip test that measures departures from unimodality
217 (Hartigan & Hartigan 1985).

218 To evaluate if the system is near a critical transition, we calculate the fluctuations of the largest patch
219 $\Delta S_{max} = S_{max}(t) - \langle S_{max} \rangle$, using the same formula for RS_{max} . To characterize fluctuations we fitted
220 three empirical distributions: power-law, log-normal, and exponential, using the same methods described
221 previously. We expect that large fluctuation near a critical point have heavy tails (log-normal or power-law)
222 and that fluctuations far from a critical point have exponential tails, corresponding to Gaussian processes
223 (Rooij *et al.* 2013). We also apply likelihood ratio test explained previously (Vuong 1989; Clauset *et al.*
224 2009); if the p-values obtained to compare the best distribution against the others are not significant we
225 concluded that there is not enough data to decide which is the best model. We generated animated maps
226 showing the fluctuations of the two largest patches at 30% threshold, to aid in the interpretations of the
227 results.

228 A robust way to detect if the system is near a critical transition is to analyze the increase in variance of the
229 density (Benedetti-Cecchi *et al.* 2015)—in our case ‘density’ is the total forest cover divided by the area.
230 It has been demonstrated that the variance increase in density appears when the system is very close to
231 the transition (Corrado *et al.* 2014), and thus practically it does not constitute an early warning indicator.
232 An alternative is to analyze the variance of the fluctuations of the largest patch ΔS_{max} : the maximum is
233 attained at the critical point but a significant increase occurs well before the system reaches the critical point
234 (Corrado *et al.* 2014; Saravia & Momo 2017). In addition, before the critical fragmentation, the skewness
235 of the distribution of ΔS_{max} should be negative, implying that fluctuations below the average are more
236 frequent. We characterized the increase in the variance using quantile regression: if variance is increasing
237 the slopes of upper or/and lower quartiles should be positive or negative.

238 All statistical analyses were performed using the GNU R version 3.3.0 (R Core Team 2015), to fit the
239 distributions of patch sizes we used the Python package powerlaw (Alstott *et al.* 2014). For the quantile
240 regressions we used the R package quantreg (Koenker 2016). Image processing was done in MATLAB r2015b
241 (The Mathworks Inc.). The complete source code for image processing and statistical analysis, and the patch

242 size data files are available at figshare <http://dx.doi.org/10.6084/m9.figshare.4263905>.

243 Results

244 The figure 1 shows an example of the distribution of the biggest 200 patches for years 2000 and 2014. This
245 distribution is highly variable; the biggest patch usually maintains its spatial location, but sometimes it
246 breaks and then big temporal fluctuations in its size are observed, as we will analyze below. Smaller patches
247 can merge or break more easily so they enter or leave the list of 200, and this is why there is a color change
248 across years.

249 The power law distribution was selected as the best model in 99% of the cases (Figure S7). In a small
250 number of cases (1%) the power law with exponential cutoff was selected, but the value of the parameter α
251 was similar by ± 0.03 to the pure power law (Table S1, and model fit data table). Additionally the patch size
252 where the exponential tail begins is very large, and thus we used the power law parameters for these cases
253 (region EUAS3,SAST2). In finite-size systems the favored model should be the power law with exponential
254 cut-off, because the power-law tails are truncated to the size of the system (Stauffer & Aharony 1994). This
255 implies that differences between the two kinds of power law models should be small. We observe this effect:
256 when the pure power-law model is selected as the best model the likelihood ratio test shows that in 64% of
257 the cases the differences with power law with exponential cutoff are not significant ($p\text{-value}>0.05$); in these
258 cases the differences between the fitted α for both models are less than 0.001. Instead the likelihood ratio
259 test clearly differentiates the power law model from the exponential model (100% cases $p\text{-value}<0.05$), and
260 the log-normal model (90% cases $p\text{-value}<0.05$).

261 The global mean of the power-law exponent α is 1.967 and the bootstrapped 95% confidence interval is
262 1.964 - 1.970. The global values for each threshold are different, because their confidence intervals do not
263 overlap, and their range goes from 1.90 to 2.01 (Table S1). Analyzing the biggest regions (Figure 1, Table
264 S2) the northern hemisphere regions (EUAS1 & NA1) have similar values of α (1.97, 1.98), pantropical areas
265 have different α with greatest values for South America (SAST1, 2.01) and in descending order Africa (AF1,
266 1.946) and Southeast Asia (SEAS1, 1.895). With greater α the fluctuations of patch sizes are lower and vice
267 versa (Newman 2005).

268 We calculated the total areas of forest and the largest patch S_{max} by year for different thresholds, and as
269 expected these two values increase for smaller thresholds (Table S3). We expect fewer variations in the
270 largest patch relative to total forest area RS_{max} (Figure S9); in ten cases it stayed near or higher than 60%
271 (EUAS2, NA5, OC2, OC3, OC4, OC5, OC6, OC8, SAST1, SAT1) over the 25-35 range or more. In four

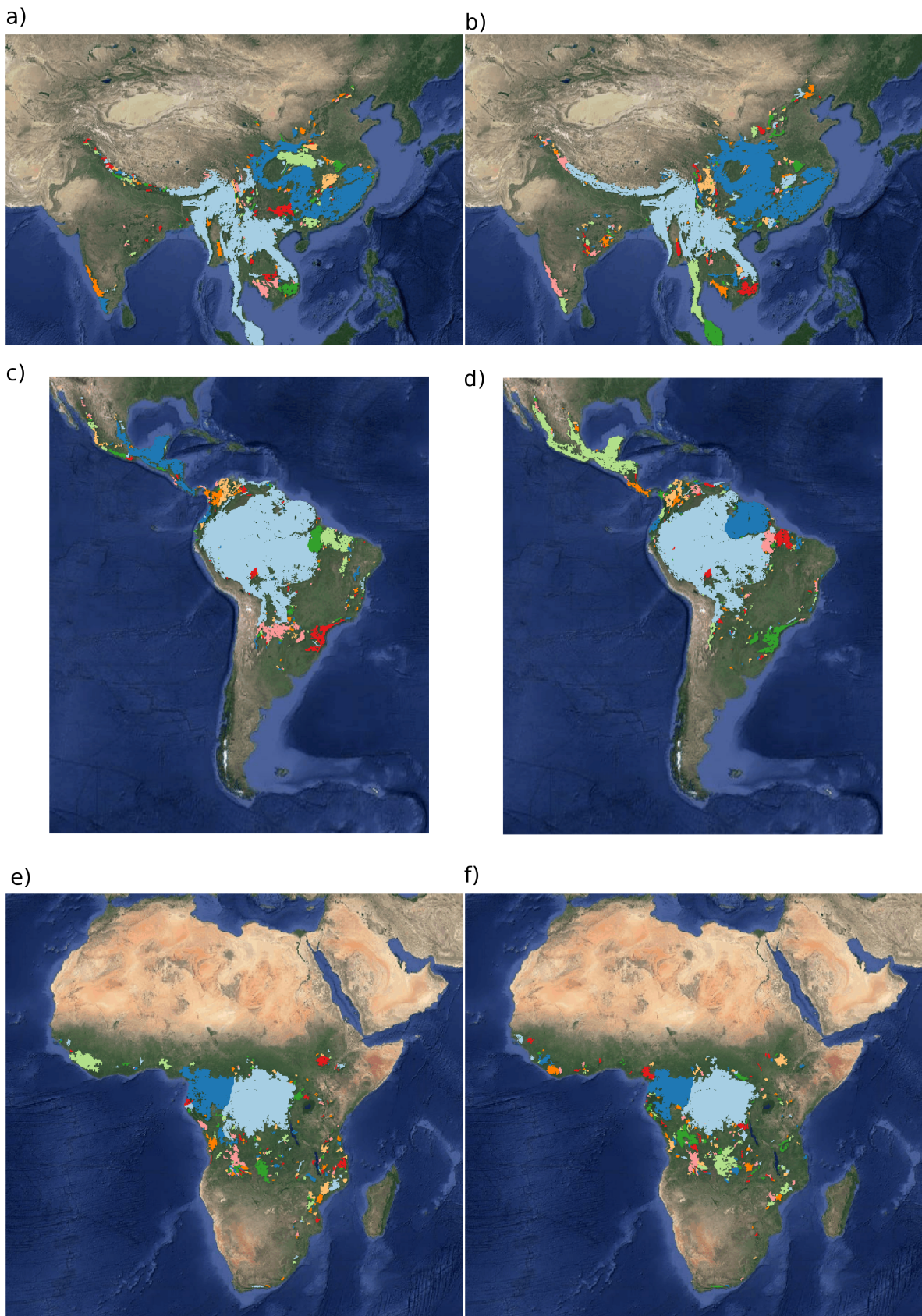


Figure 1: Forest patch distributions for continental regions for the years 2000 and 2014. The images are the 200 biggest patches, shown at a coarse pixel scale of 2.5 km. The regions are: a) & b) southeast Asia; c) & d) South America subtropical and tropical and e) & f) Africa mainland, for the years 2000 and 2014 respectively. The color palette was chosen to discriminate different patches and does not represent patch size.

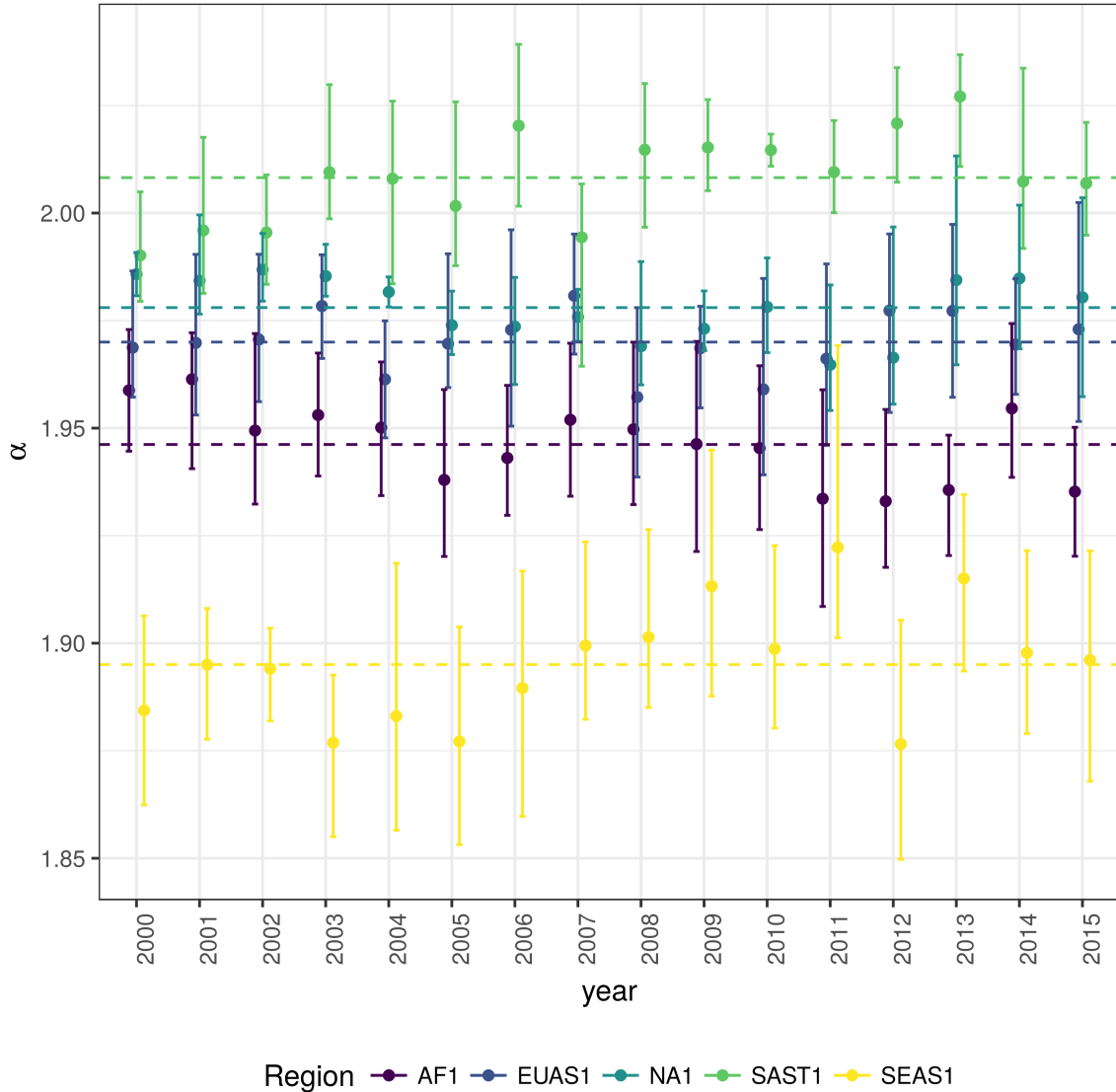


Figure 2: Power law exponents (α) of forest patch distributions for regions with total forest area $> 10^7 \text{ km}^2$. Dashed horizontal lines are the means by region, with 95% confidence interval error bars estimated by bootstrap resampling. The regions are AF1: Africa mainland, EUAS1: Eurasia mainland, NA1: North America mainland, SAST1: South America subtropical and tropical, SEAS1: Southeast Asia mainland.

272 cases it stayed around 40% or less, at least over the 25-30% range (AF1, EUAS3, OC1, SAST2), and in six
273 cases there is a crossover from more than 60% to around 40% or less (AF2, EUAS1, NA1, OC7, SEAS1,
274 SEAS2). This confirms the criteria of using the most conservative threshold value of 40% to interpret RS_{max}
275 with regard to the fragmentation state of the forest. The frequency of RS_{max} showed bimodality (Figure
276 S10) and the dip test rejected unimodality ($D = 0.0416$, p -value = 0.0003), which also implies that RS_{max}
277 is a good index to study the fragmentation state of the forest.

278 The RS_{max} for regions with more than 10^7 km 2 of forest is shown in figure 3. South America tropical and
279 subtropical (SAST1) is the only region with an average close to 60%, the other regions are below 30%. Eurasia
280 mainland (EUAS1) has the lowest value near 20%. For regions with less total forest area (Figure S10, Table
281 S3), Great Britain (EUAS3) has the lowest proportion less than 5%, Java (OC7) and Cuba (SAST2) are
282 under 25%, while other regions such as New Guinea (OC2), Malaysia/Kalimantan (OC3), Sumatra (OC4),
283 Sulawesi (OC5) and South New Zealand (OC6) have a very high proportion (75% or more). Philippines
284 (SEAS2) seems to be a very interesting case because it seems to be under 30% until the year 2007, fluctuates
285 around 30% in years 2008-2010, then jumps near 60% in 2011-2013 and then falls again to 30%, this seems
286 an example of a transition from a fragmented state to a unfragmented one (figure S11).

287 We analyzed the distributions of fluctuations of the largest patch relative to total forest area ΔRS_{max} and
288 the fluctuations of the largest patch ΔS_{max} . Although the Akaike criteria identified different distributions
289 as the best, in most cases the Likelihood ratio test was not significant and we are not able, from these data,
290 to determine with confidence which is the best distribution. In only one case was the distribution selected
291 by the Akaike criteria confirmed as the correct model for relative and absolute fluctuations (Table S4).

292 The animations of the two largest patches (see supplementary data, largest patch gif animations) qualitatively
293 shows the nature of fluctuations and if the state of the forest is connected or not. If the largest patch is
294 always the same patch over time, the forest is probably not fragmented; this happens for regions with RS_{max}
295 of more than 40% such as AF2 (Madagascar), EUAS2 (Japan), NA5 (Newfoundland) and OC3 (Malaysia).
296 In regions with RS_{max} between 40% and 30% the identity of the largest patch could change or stay the
297 same in time. For OC7 (Java) the largest patch changes and for AF1 (Africa mainland) it stays the same.
298 Only for EUAS1 (Eurasia mainland) we observed that the two largest patches are always the same, implying
299 that these two large patches are probably by a geographical accident but they have the same dynamics. The
300 regions with RS_{max} less than 25% (SAST2-Cuba and EUAS3-Great Britain) have a always-changing largest
301 patch reflecting their fragmented state. In the case of SEAS2 (Philippines) a transition is observed, with the
302 identity of the largest patch first variable, and then constant after 2010.

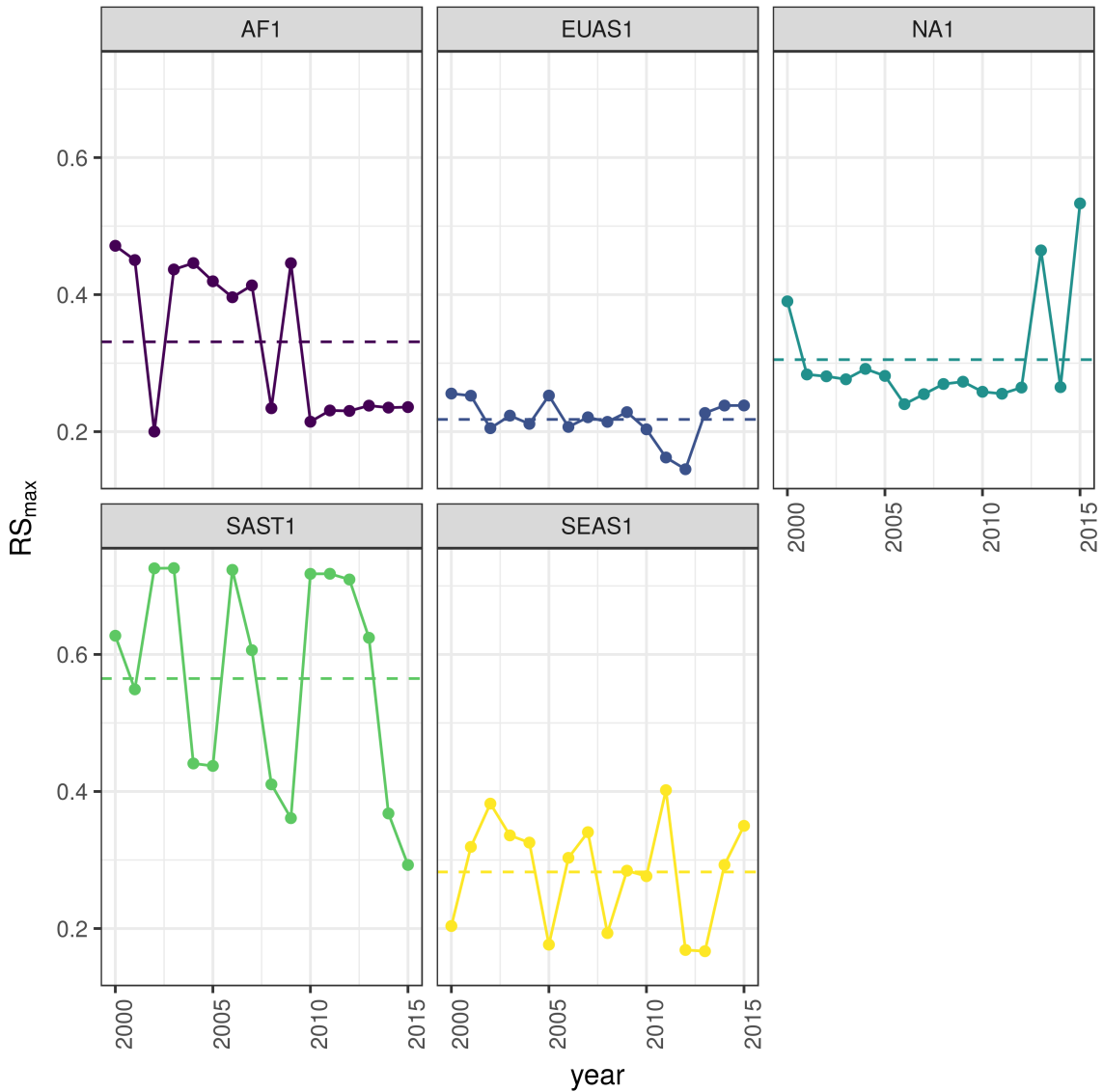


Figure 3: Largest patch proportion relative to total forest area RS_{max} , for regions with total forest area $> 10^7 \text{ km}^2$. We show here the RS_{max} calculated using a threshold of 40% of forest in each pixel to determine patches. Dashed lines are averages across time. The regions are AF1: Africa mainland, EUAS1: Eurasia mainland, NA1: North America mainland, SAST1: South America tropical and subtropical, SEAS1: Southeast Asia mainland.

303 The results of quantile regressions are almost identical for ΔRS_{max} and ΔS_{max} (table S5). Among the biggest
304 regions, Africa (AF1) has a similar pattern across thresholds but only the 30% threshold is significant; the
305 upper and lower quantiles have significant negative slopes, but the lower quantile slope is lower, implying
306 that negative fluctuations and variance are increasing (Figure 4). Eurasia mainland (EUAS1) has significant
307 slopes at 20%, 30% and 40% thresholds but the patterns are different at 20% variance is decreasing, at 30%
308 and 40% only is increasing. Thus the variation of the most dense portion of the largest patch is increasing
309 within a limited range. North America mainland (NA1) exhibits the same pattern at 20%, 25% and 30%
310 thresholds: a significant lower quantile with positive slope, implying decreasing variance. South America
311 tropical and subtropical (SAST1) have significant lower quantile with a negative slope at 25% and 30%
312 thresholds indicating an increase in variance. SEAS1 has an upper quantile with positive slope significant
313 for 25% threshold, also indicating an increasing variance. The other regions, with forest area smaller than
314 10^7 km^2 are shown in figure S11 and table S5. Philippines (SEAS2) is an interesting case: the slopes of lower
315 quantiles are positive for thresholds 20% and 25%, and the upper quantile slopes are positive for thresholds
316 30% and 40%; thus variance is decreasing at 20%-25% and increasing at 30%-40%.

317 The conditions that indicate that a region is near a critical fragmentation threshold are that patch size
318 distributions follow a power law; variance of ΔRS_{max} is increasing in time; and skewness is negative. All
319 these conditions must happen at the same time at least for one threshold. When the threshold is higher more
320 dense regions of the forest are at risk. This happens for Africa mainland (AF1), Eurasia mainland(EUAS1),
321 Japan (EUAS2), Australia mainland (OC1), Malaysia/Kalimantan (OC3), Sumatra (OC4), South America
322 tropical & subtropical (SAST1), Cuba (SAST2), Southeast Asia, Mainland (SEAS1).

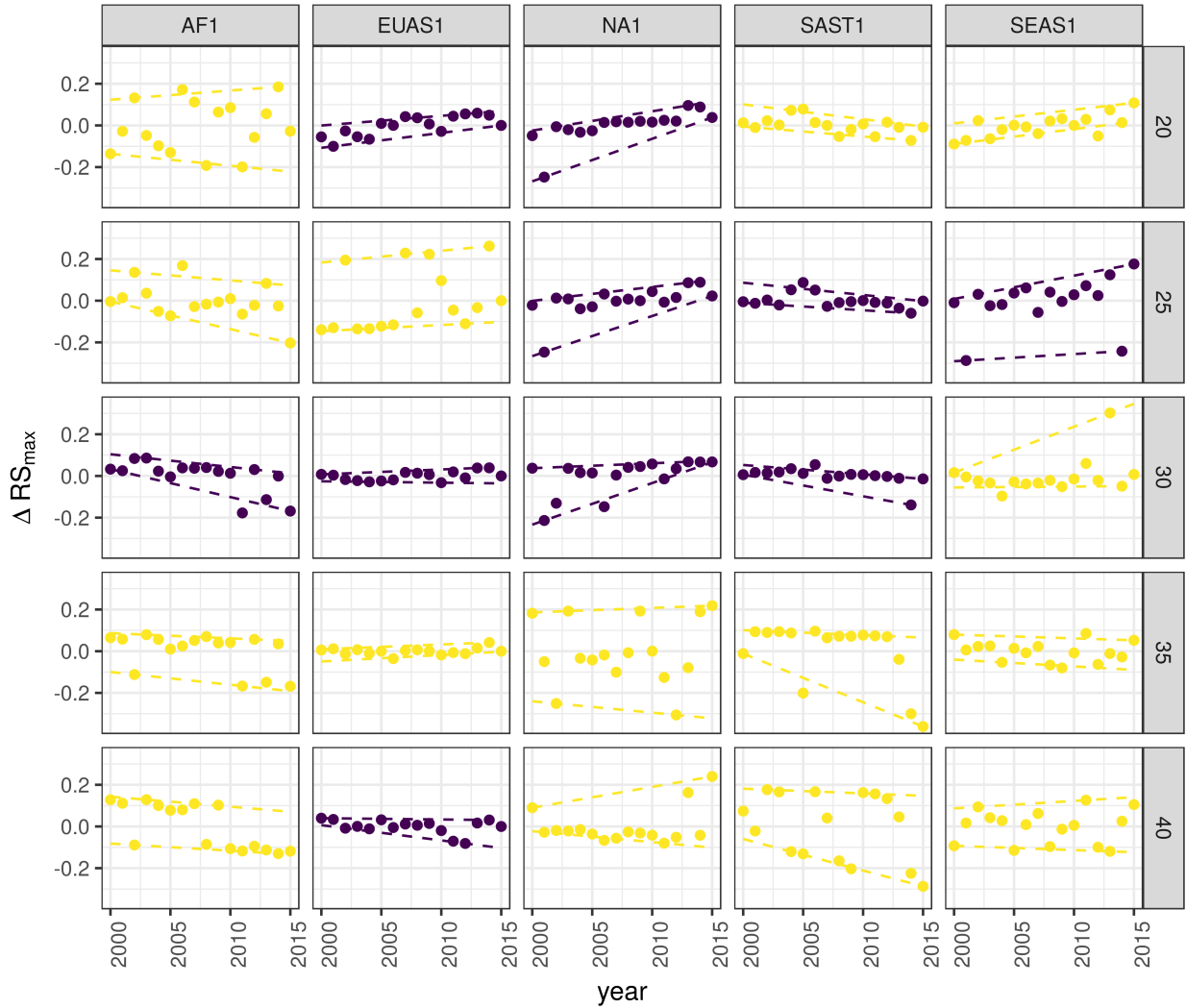


Figure 4: Largest patch fluctuations for regions with total forest area $> 10^7 \text{ km}^2$ across years. The patch sizes are relative to the total forest area of the same year. Dashed lines are 90% and 10% quantile regressions, to show if fluctuations were increasing; purple (dark) panels have significant slopes. The regions are AF1: Africa mainland, EUAS1: Eurasia mainland, NA1: North America mainland, SAST1: South America tropical and subtropical, SEAS1: Southeast Asia mainland.

Table 1: Regions and indicators of closeness to a critical fragmentation point. Where: RS_{max} is the largest patch divided by the total forest area; Threshold is the value used to calculate patches from the MODIS VCF pixels; ΔRS_{max} are the fluctuations of RS_{max} around the mean and the increase or decrease in the variance was estimated using quantile regressions; skewness was calculated for RS_{max} . NS means the results were non-significant. The conditions that determine the closeness to a fragmentation point are: increasing variance of ΔRS_{max} and negative skewness. RS_{max} indicates if the forest is unfragmented (>0.6) or fragmented (<0.3).

Region	Description	RS_{max}	Threshold	Variance of ΔRS_{max}	Skewness
AF1	Africa mainland	0.33	30	Increase	-1.4653
AF2	Madagascar	0.48	20	Increase	0.7226
EUAS1	Eurasia, mainland	0.22	20	Decrease	-0.4814
EUAS1			30	Increase	0.3113
EUAS1			40	Increase	-1.2790
EUAS2	Japan	0.94	35	Increase	-0.3913
EUAS2			40	Increase	-0.5030
EUAS3	Great Britain	0.03	40	NS	
NA1	North America, mainland	0.31	20	Decrease	-2.2895
NA1			25	Decrease	-2.4465
NA1			30	Decrease	-1.6340
NA5	Newfoundland	0.54	40	NS	
OC1	Australia, Mainland	0.36	30	Increase	0.0920
OC1			35	Increase	-0.8033
OC2	New Guinea	0.96	25	Decrease	-0.1003
OC2			30	Decrease	0.1214
OC2			35	Decrease	-0.0124
OC3	Malaysia/Kalimantan	0.92	35	Increase	-1.0147
OC3			40	Increase	-1.5649
OC4	Sumatra	0.84	20	Increase	-1.3846
OC4			25	Increase	-0.5887
OC4			30	Increase	-1.4226
OC5	Sulawesi	0.82	40	NS	
OC6	New Zealand South Island	0.75	40	Increase	0.3553
OC7	Java	0.16	40	NS	
OC8	New Zealand North Island	0.64	40	NS	
SAST1	South America, Tropical and Subtropical forest	0.56	25	Increase	1.0519
SAST1			30	Increase	-2.7216
SAST2	Cuba	0.15	20	Increase	0.5049
SAST2			25	Increase	1.7263
SAST2			30	Increase	0.1665
SAST2			40	Increase	-0.5401
SAT1	South America, Temperate forest	0.54	25	Decrease	0.1483
SAT1			30	Decrease	-1.6059
SAT1			35	Decrease	-1.3809
SEAS1	Southeast Asia, Mainland	0.28	25	Increase	-1.3328
SEAS2	Philippines	0.33	20	Decrease	-1.6373
SEAS2			25	Decrease	-0.6648
SEAS2			30	Increase	0.1517

Region	Description	RS_{max}	Threshold	Variance of ΔRS_{max}	Skewness
SEAS2			40	Increase	1.5996

323 Discussion

324 We found that the forest patch distribution of all regions of the world, spanning tropical rainforests, boreal
 325 and temperate forests, followed power laws spanning seven orders of magnitude. Power laws have previously
 326 been found for several kinds of vegetation, but never at global scales as in this study. Moreover, the range
 327 of the estimated power law exponents is relatively narrow (1.90 - 2.01), even though we tested a variety
 328 of different thresholds levels. This suggests the existence of one unifying mechanism, or perhaps different
 329 mechanisms that act in the same way in different regions, affecting forest spatial structure and dynamics.

330 Several mechanisms have been proposed for the emergence of power laws in forests. The first is related self
 331 organized criticality (SOC), when the system is driven by its internal dynamics to a critical state; this has
 332 been suggested mainly for fire-driven forests (Zinck & Grimm 2009; Hantson *et al.* 2015). Real ecosystems
 333 do not seem to meet the requirements of SOC dynamics (Pueyo *et al.* 2010; McKenzie & Kennedy 2012),
 334 however, because they have both endogenous and exogenous controls, are non-homogeneous, and do not
 335 have a separation of time scales (Solé *et al.* 2002; Solé & Bascompte 2006). A second possible mechanism,
 336 suggested by Pueyo *et al.* (2010), is isotropic percolation: when a system is near the critical point, the power
 337 law structures arise. This is equivalent to the random forest model that we explained previously, and requires
 338 the tuning of an external environmental condition to carry the system to this point. We did not expect forest
 339 growth to be a random process at local scales, but it is possible that combinations of factors cancel out to
 340 produce seemingly random forest dynamics at large scales. This has been suggested as a mechanism for the
 341 observed power laws of global tropical forest at year 2000 (Taubert *et al.* 2018). In this case we should have
 342 observed power laws in a limited set of situations that coincide with a critical point, but instead we observed
 343 pervasive power law distributions. Thus isotropic percolation does not seem likely to be the mechanism that
 344 produces the observed distributions.

345 A third possible mechanism is facilitation (Manor & Shnerb 2008; Irvine *et al.* 2016): a patch surrounded
 346 by forest will have a smaller probability of being deforested or degraded than an isolated patch. The model
 347 of Scanlon *et al.* (2007) showed an $\alpha = 1.34$ which is different from our results (1.90 - 2.01 range). Another
 348 model but with three states (tree/non-tree/degraded), including local facilitation and grazing, was also used
 349 to obtain power laws patch distributions without external tuning, and exhibited deviations from power laws
 350 at high grazing pressures (Kéfi *et al.* 2007). The values of the power law exponent α obtained for this model

351 are dependent on the intensity of facilitation: when facilitation is more intense the exponent is higher, but
352 the maximal values they obtained are still lower than the ones we observed. Thus an exploration of the
353 parameters of this model and simulations at a continental scale will be needed to find if this is a plausible
354 mechanism.

355 It has been suggested that a combination of spatial and temporal indicators could more reliably detect critical
356 transitions (Kéfi *et al.* 2014). In this study, we combined five criteria to evaluate the closeness of the system
357 to a fragmentation threshold. Two of them were spatial: the forest patch size distribution, and the proportion
358 of the largest patch relative to total forest area RS_{max} . The other three were the distribution of temporal
359 fluctuations in the largest patch size, the trend in the variance, and the skewness of the fluctuations. One
360 of them: the distribution of temporal fluctuations ΔRS_{max} can not be applied with our temporal resolution
361 due to the difficulties of fitting and comparing heavy tailed distributions. The combination of the remaining
362 four gives us an increased degree of confidence about the system being close to a critical transition.

363 Monitoring the biggest patches using RS_{max} is also important regardless of the existence or not of critical
364 transitions. RS_{max} is relative to total forest area thus it could be used to compare regions with a different
365 extension of forests and as the total area of forest also changes with different environmental conditions,
366 e.g. this could be used to compare forest from different latitudes. Moreover, the areas covered by S_{max}
367 across regions contain most of the intact forest landscapes defined by Potapov *et al.* (2008b), and thus
368 RS_{max} is a relatively simple way to evaluate the risk in these areas.

369 South America tropical and subtropical (SAST1), Southeast Asia mainland (SEAS1) and Africa mainland
370 (AF1) met all criteria at least for one threshold; these regions generally experience the biggest rates of
371 deforestation with a significant increase in loss of forest (Hansen *et al.* 2013). From our point of view the
372 most critical region is Southeast Asia, because the proportion of the largest patch relative to total forest
373 area RS_{max} was 28%. This suggests that Southeast Asia's forests are the most fragmented, and thus its
374 flora and fauna the most endangered. Due to the criteria we adopted to define regions, we could not detect
375 the effect of conservation policies applied at a country level, e.g. the Natural Forest Conservation Program
376 in China, which has produced an 1.6% increase in forest cover and net primary productivity over the last 20
377 years (Viña *et al.* 2016). Indonesia and Malaysia (OC3) both are countries with hight deforestation rates
378 (Hansen *et al.* 2013); Sumatra (OC4) is the biggest island of Indonesia and where most deforestation occurs.
379 Both regions show a high RS_{max} greater than 60%, and thus the forest is in an unfragmented state, but
380 they met all other criteria, meaning that they are approaching a transition if the actual deforestation rates
381 continue.

382 The Eurasian mainland region (EUAS1) is an extensive area with mainly temperate and boreal forest, and a
383 combination of forest loss due to fire (Potapov *et al.* 2008a) and forestry. The biggest country is Russia that
384 experienced the biggest rate of forest loss of all countries, but here in the zone of coniferous forest the the
385 largest gain is observed due to agricultural abandonment (Prishchepov *et al.* 2013). The loss is maximum
386 at the most dense areas of forest (Hansen *et al.* 2013, Table S3), this coincides with our analysis that detect
387 an increasing risk at denser forest. This region also has a relatively low RS_{max} that means is probably near
388 a fragmented state. A region that is similar in forest composition to EAUS1 is North America (NA1); the
389 two main countries involved, United States and Canada, have forest dynamics mainly influenced by fire and
390 forestry, with both regions are extensively managed for industrial wood production. North America has a
391 higher RS_{max} than Eurasia and a positive skewness that excludes it from being near a critical transition. A
392 possible explanation of this is that in Russia after the collapse of the Soviet Union harvest was lower due to
393 agricultural abandonment but illegal overharvesting of high valued stands has increased in recent decades
394 (Gauthier *et al.* 2015).

395 The analysis of RS_{max} reveals that the island of Philippines (SEAS2) seems to be an example of a critical
396 transition from an unconnected to a connected state, i.e. from a state with high fluctuations and low RS_{max}
397 to a state with low fluctuations and high RS_{max} . If we observe this pattern backwards in time, the decrease
398 in variance become an increase, and negative skewness is constant, and thus the region exhibits the criteria
399 of a critical transition (Table 1, Figure S12). The actual pattern of transition to an unfragmented state
400 could be the result of an active intervention of the government promoting conservation and rehabilitation
401 of protected areas, ban of logging old-growth forest, reforestation of barren areas, community-based forestry
402 activities, and sustainable forest management in the country's production forest (Lasco *et al.* 2008). This
403 confirms that the early warning indicators proposed here work in the correct direction. An important caveat
404 is that the MODIS dataset does not detect if native forest is replaced by agroindustrial tree plantations like
405 oil palms, that are among the main drivers of deforestation in this area (Malhi *et al.* 2014). To improve
406 the estimation of forest patches, data sets as the MODIS cropland probability and others about land use,
407 protected areas, forest type, should be incorporated (Hansen *et al.* 2014; Sexton *et al.* 2015).

408 Deforestation and fragmentation are closely related. At low levels of habitat reduction species population
409 will decline proportionally; this can happen even when the habitat fragments retain connectivity. As habitat
410 reduction continues, the critical threshold is approached and connectivity will have large fluctuations (Brook
411 *et al.* 2013). This could trigger several negative synergistic effects: population fluctuations and the possibility
412 of extinctions will rise, increasing patch isolation and decreasing connectivity (Brook *et al.* 2013). This
413 positive feedback mechanism will be enhanced when the fragmentation threshold is reached, resulting in the

loss of most habitat specialist species at a landscape scale (Pardini *et al.* 2010). Some authors have argued that since species have heterogeneous responses to habitat loss and fragmentation, and biotic dispersal is limited, the importance of thresholds is restricted to local scales or even that its existence is questionable (Brook *et al.* 2013). Fragmentation is by definition a local process that at some point produces emergent phenomena over the entire landscape, even if the area considered is infinite (Oborny *et al.* 2005). If a forest is already in a fragmented state, a second critical transition from forest to non-forest could happen: the desertification transition (Corrado *et al.* 2014). Considering the actual trends of habitat loss, and studying the dynamics of non-forest patches—instead of the forest patches as we did here—the risk of this kind of transition could be estimated. The simple models proposed previously could also be used to estimate if these thresholds are likely to be continuous and reversible or discontinuous and often irreversible (Weissmann & Shnerb 2016), and the degree of protection (e.g. using the set-asides strategy Banks-Leite *et al.* (2014)) that would be necessary to stop this trend.

The effectiveness of landscape management is related to the degree of fragmentation, and the criteria to direct reforestation efforts could be focused on regions near a transition (Oborny *et al.* 2007). Regions that are in an unconnected state require large efforts to recover a connected state, but regions that are near a transition could be easily pushed to a connected state; feedbacks due to facilitation mechanisms might help to maintain this state. Crossing the fragmentation critical point in forests could have negative effects on biodiversity and ecosystem services (Haddad *et al.* 2015), but it could also produce feedback loops at different levels of the biological hierarchy. This means that a critical transition produced at a continental scale could have effects at the level of communities, food webs, populations, phenotypes and genotypes (Barnosky *et al.* 2012). All these effects interact with climate change, thus there is a potential production of cascading effects that could lead to an abrupt climate change with potentially large ecological and economic impact (Alley *et al.* 2003).

Therefore, even if critical thresholds are reached only in some forest regions at a continental scale, a cascading effect with global consequences could still be produced (Reyer *et al.* 2015). The risk of such event will be higher if the dynamics of separate continental regions are coupled (Lenton & Williams 2013). At least three of the regions defined here are considered tipping elements of the earth climate system that could be triggered during this century (Lenton *et al.* 2008). These were defined as policy relevant tipping elements so that political decisions could determine whether the critical value is reached or not. Thus the criteria proposed here could be used as a more sensitive system to evaluate the closeness of a tipping point at a continental scale. Further improvements will produce quantitative predictions about the temporal horizon where these critical transitions could produce significant changes in the studied systems.

445 **Supporting information**

446 **Appendix**

447 *Table S1:* Mean power-law exponent and Bootstrapped 95% confidence intervals by threshold.

448 *Table S2:* Mean power-law exponent and Bootstrapped 95% confidence intervals across thresholds by region
449 and year.

450 *Table S3:* Mean total patch area; largest patch S_{max} in km²; largest patch relative to total patch area RS_{max}
451 and 95% bootstrapped confidence interval of RS_{max} , by region and thresholds, averaged across years

452 *Table S4:* Model selection for distributions of fluctuation of largest patch ΔS_{max} and largest patch relative
453 to total forest area ΔRS_{max} .

454 *Table S5:* Quantil regressions of the fluctuations of the largest patch vs year, for 10% and 90% quantils at
455 different pixel thresholds.

456 *Table S6:* Unbiased estimation of Skewness of fluctuations of the largest patch ΔS_{max} and fluctuations
457 relative to total forest area ΔRS_{max} .

458 *Figure S1:* Regions for Africa: Mainland (AF1), Madagascar (AF2).

459 *Figure S2:* Regions for Eurasia: Mainland (EUAS1), Japan (EUAS2), Great Britain (EUAS3).

460 *Figure S3:* Regions for North America: Mainland (NA1), Newfoundland (NA5).

461 *Figure S4:* Regions for Australia and islands: Australia mainland (OC1), New Guinea (OC2),
462 Malaysia/Kalimantan (OC3), Sumatra (OC4), Sulawesi (OC5), New Zealand south island (OC6),
463 Java (OC7), New Zealand north island (OC8).

464 *Figure S5:* Regions for South America: Tropical and subtropical forest up to Mexico (SAST1), Cuba
465 (SAST2), South America Temperate forest (SAT1).

466 *Figure S6:* Regions for Southeast Asia: Mainland (SEAS1), Philippines (SEAS2).

467 *Figure S7:* Proportion of best models selected for patch size distributions using the Akaike criterion.

468 *Figure S8:* Power law exponents for forest patch distributions by year for all regions.

469 *Figure S9:* Average largest patch relative to total forest area RS_{max} by threshold, for all regions.

470 *Figure s10:* Frequency distribution of Largest patch proportion relative to total forest area RS_{max} calculated
471 using a threshold of 40%.

472 *Figure S11:* Largest patch relative to total forest area RS_{max} by year at 40% threshold, for regions with
473 total forest area less than 10^7 km^2 .

474 *Figure S12:* Fluctuations of largest patch relative to total forest area RS_{max} for regions with total forest
475 area less than 10^7 km^2 by year and threshold.

476 Data Accessibility

477 The MODIS VCF product is freely available from NASA at <https://search.earthdata.nasa.gov/>. Csv text file
478 with model fits for patch size distribution, and model selection for all the regions; Gif Animations of a forest
479 model percolation; Gif animations of largest patches; patch size files for all years and regions used here; and all
480 the R, Python and Matlab scripts are available at figshare <http://dx.doi.org/10.6084/m9.figshare.4263905>.

481 Acknowledgments

482 LAS and SRD are grateful to the National University of General Sarmiento for financial support. We want to
483 thank to Jordi Bascompte, Nara Guisoni, Fernando Momo, and two anonymous reviewers for their comments
484 and discussions that greatly improved the manuscript. This work was partially supported by a grant from
485 CONICET (PIO 144-20140100035-CO).

486 References

- 487 Alley, R.B., Marotzke, J., Nordhaus, W.D., Overpeck, J.T., Peteet, D.M. & Pielke, R.A. *et al.* (2003).
488 Abrupt Climate Change. *Science*, 299, 2005–2010.
- 489 Allington, G.R.H. & Valone, T.J. (2010). Reversal of desertification: The role of physical and chemical soil
490 properties. *Journal of Arid Environments*, 74, 973–977.
- 491 Alstott, J., Bullmore, E. & Plenz, D. (2014). powerlaw: A Python Package for Analysis of Heavy-Tailed
492 Distributions. *PLOS ONE*, 9, e85777.
- 493 Angelsen, A. (2010). Policies for reduced deforestation and their impact on agricultural production. *Pro-*
494 *ceedings of the National Academy of Sciences*, 107, 19639–19644.
- 495 Banks-Leite, C., Pardini, R., Tambosi, L.R., Pearse, W.D., Bueno, A.A. & Bruscagin, R.T. *et al.* (2014).
496 Using ecological thresholds to evaluate the costs and benefits of set-asides in a biodiversity hotspot. *Science*,

- 497 345, 1041–1045.
- 498 Barnosky, A.D., Hadly, E.A., Bascompte, J., Berlow, E.L., Brown, J.H. & Fortelius, M. *et al.* (2012).
499 Approaching a state shift in Earth’s biosphere. *Nature*, 486, 52–58.
- 500 Bascompte, J. & Solé, R.V. (1996). Habitat fragmentation and extinction thresholds in spatially explicit
501 models. *Journal of Animal Ecology*, 65, 465–473.
- 502 Bazant, M.Z. (2000). Largest cluster in subcritical percolation. *Physical Review E*, 62, 1660–1669.
- 503 Belward, A.S. (1996). *The IGBP-DIS Global 1 Km Land Cover Data Set “DISCover”: Proposal and*
504 *Implementation Plans : Report of the Land Recover Working Group of IGBP-DIS*. IGBP-dis working paper.
505 IGBP-DIS Office.
- 506 Benedetti-Cecchi, L., Tamburello, L., Maggi, E. & Bulleri, F. (2015). Experimental Perturbations Modify
507 the Performance of Early Warning Indicators of Regime Shift. *Current biology*, 25, 1867–1872.
- 508 Bestelmeyer, B.T., Duniway, M.C., James, D.K., Burkett, L.M. & Havstad, K.M. (2013). A test of critical
509 thresholds and their indicators in a desertification-prone ecosystem: more resilience than we thought. *Ecology*
510 *Letters*, 16, 339–345.
- 511 Bestelmeyer, B.T., Ellison, A.M., Fraser, W.R., Gorman, K.B., Holbrook, S.J. & Laney, C.M. *et al.* (2011).
512 Analysis of abrupt transitions in ecological systems. *Ecosphere*, 2, 129.
- 513 Boettiger, C. & Hastings, A. (2012). Quantifying limits to detection of early warning for critical transitions.
514 *Journal of The Royal Society Interface*, 9, 2527–2539.
- 515 Bonan, G.B. (2008). Forests and Climate Change: Forcings, Feedbacks, and the Climate Benefits of Forests.
516 *Science*, 320, 1444–1449.
- 517 Botet, R. & Ploszajczak, M. (2004). Correlations in Finite Systems and Their Universal Scaling Properties.
518 In: *Nonequilibrium physics at short time scales: Formation of correlations* (ed. Morawetz, K.). Springer-
519 Verlag, Berlin Heidelberg, pp. 445–466.
- 520 Brook, B.W., Ellis, E.C., Perring, M.P., Mackay, A.W. & Blomqvist, L. (2013). Does the terrestrial biosphere
521 have planetary tipping points? *Trends in Ecology & Evolution*.
- 522 Burnham, K. & Anderson, D.R. (2002). *Model selection and multi-model inference: A practical information-*
523 *theoretic approach*. 2nd. edn. Springer-Verlag, New York.
- 524 Canfield, D.E., Glazer, A.N. & Falkowski, P.G. (2010). The Evolution and Future of Earth’s Nitrogen Cycle.

- 525 Carpenter, S.R., Cole, J.J., Pace, M.L., Batt, R., Brock, W.A. & Cline, T. *et al.* (2011). Early Warnings of
526 Regime Shifts: A Whole-Ecosystem Experiment. *Science*, 332, 1079–1082.
- 527
- 528 Clauset, A., Shalizi, C. & Newman, M. (2009). Power-Law Distributions in Empirical Data. *SIAM Review*,
529 51, 661–703.
- 530 Corrado, R., Cherubini, A.M. & Pennetta, C. (2014). Early warning signals of desertification transitions in
531 semiarid ecosystems. *Physical Review E - Statistical, Nonlinear, and Soft Matter Physics*, 90, 62705.
- 532 Crawley, M.J. (2012). *The R Book*. 2nd. edn. Wiley, Hoboken, NJ, USA.
- 533 Crowther, T.W., Glick, H.B., Covey, K.R., Bettigole, C., Maynard, D.S. & Thomas, S.M. *et al.* (2015).
534 Mapping tree density at a global scale. *Nature*, 525, 201–205.
- 535 Dai, L., Vorselen, D., Korolev, K.S. & Gore, J. (2012). Generic Indicators for Loss of Resilience Before a
536 Tipping Point Leading to Population Collapse. *Science*, 336, 1175–1177.
- 537 DiMiceli, C., Carroll, M., Sohlberg, R., Huang, C., Hansen, M. & Townshend, J. (2015). Annual Global
538 Automated MODIS Vegetation Continuous Fields (MOD44B) at 250 m Spatial Resolution for Data Years
539 Beginning Day 65, 2000 - 2014, Collection 051 Percent Tree Cover, University of Maryland, College Park,
540 MD, USA.
- 541 Drake, J.M. & Griffen, B.D. (2010). Early warning signals of extinction in deteriorating environments.
542 *Nature*, 467, 456–459.
- 543 Efron, B. & Tibshirani, R.J. (1994). *An Introduction to the Bootstrap*. Chapman & hall/crc monographs on
544 statistics & applied probability. Taylor & Francis, New York.
- 545 Filotas, E., Parrott, L., Burton, P.J., Chazdon, R.L., Coates, K.D. & Coll, L. *et al.* (2014). Viewing forests
546 through the lens of complex systems science. *Ecosphere*, 5, 1–23.
- 547 Foley, J.A., Ramankutty, N., Brauman, K.A., Cassidy, E.S., Gerber, J.S. & Johnston, M. *et al.* (2011).
548 Solutions for a cultivated planet. *Nature*, 478, 337–342.
- 549 Fung, T., O'Dwyer, J.P., Rahman, K.A., Fletcher, C.D. & Chisholm, R.A. (2016). Reproducing static and
550 dynamic biodiversity patterns in tropical forests: the critical role of environmental variance. *Ecology*, 97,
551 1207–1217.
- 552 Gardner, R.H. & Urban, D.L. (2007). Neutral models for testing landscape hypotheses. *Landscape Ecology*,

- 553 22, 15–29.
- 554 Gastner, M.T., Oborny, B., Zimmermann, D.K. & Pruessner, G. (2009). Transition from Connected to Frag-
555 mented Vegetation across an Environmental Gradient: Scaling Laws in Ecotone Geometry. *The American*
556 *Naturalist*, 174, E23–E39.
- 557 Gauthier, S., Bernier, P., Kuuluvainen, T., Shvidenko, A.Z. & Schepaschenko, D.G. (2015). Boreal forest
558 health and global change. *Science*, 349, 819 LP–822.
- 559 Gilman, S.E., Urban, M.C., Tewksbury, J., Gilchrist, G.W. & Holt, R.D. (2010). A framework for community
560 interactions under climate change. *Trends in Ecology & Evolution*, 25, 325–331.
- 561 Goldstein, M.L., Morris, S.A. & Yen, G.G. (2004). Problems with fitting to the power-law distribution. *The*
562 *European Physical Journal B - Condensed Matter and Complex Systems*, 41, 255–258.
- 563 Haddad, N.M., Brudvig, L.a., Clobert, J., Davies, K.F., Gonzalez, A. & Holt, R.D. *et al.* (2015). Habitat
564 fragmentation and its lasting impact on Earth’s ecosystems. *Science Advances*, 1, 1–9.
- 565 Hansen, M., Potapov, P., Margono, B., Stehman, S., Turubanova, S. & Tyukavina, A. (2014). Response to
566 Comment on “High-resolution global maps of 21st-century forest cover change”. *Science*, 344, 981.
- 567 Hansen, M.C., Potapov, P.V., Moore, R., Hancher, M., Turubanova, S.A. & Tyukavina, A. *et al.* (2013).
568 High-Resolution Global Maps of 21st-Century Forest Cover Change. *Science*, 342, 850–853.
- 569 Hantson, S., Pueyo, S. & Chuvieco, E. (2015). Global fire size distribution is driven by human impact and
570 climate. *Global Ecology and Biogeography*, 24, 77–86.
- 571 Harris, T.E. (1974). Contact interactions on a lattice. *The Annals of Probability*, 2, 969–988.
- 572 Hartigan, J.A. & Hartigan, P.M. (1985). The Dip Test of Unimodality. *The Annals of Statistics*, 13, 70–84.
- 573 Hastings, A. & Wysham, D.B. (2010). Regime shifts in ecological systems can occur with no warning. *Ecology*
574 *Letters*, 13, 464–472.
- 575 He, F. & Hubbell, S. (2003). Percolation Theory for the Distribution and Abundance of Species. *Physical*
576 *Review Letters*, 91, 198103.
- 577 Hinrichsen, H. (2000). Non-equilibrium critical phenomena and phase transitions into absorbing states.
578 *Advances in Physics*, 49, 815–958.
- 579 Hirota, M., Holmgren, M., Nes, E.H.V. & Scheffer, M. (2011). Global Resilience of Tropical Forest and

- 580 Savanna to Critical Transitions. *Science*, 334, 232–235.
- 581 Irvine, M.A., Bull, J.C. & Keeling, M.J. (2016). Aggregation dynamics explain vegetation patch-size distri-
582 butions. *Theoretical Population Biology*, 108, 70–74.
- 583 Keitt, T.H., Urban, D.L. & Milne, B.T. (1997). Detecting critical scales in fragmented landscapes. *Conser-
584 vation Ecology*, 1, 4.
- 585 Kéfi, S., Guttal, V., Brock, W.A., Carpenter, S.R., Ellison, A.M. & Livina, V.N. *et al.* (2014). Early
586 Warning Signals of Ecological Transitions: Methods for Spatial Patterns. *PLoS ONE*, 9, e92097.
- 587 Kéfi, S., Rietkerk, M., Alados, C.L., Pueyo, Y., Papanastasis, V.P. & ElAich, A. *et al.* (2007). Spatial
588 vegetation patterns and imminent desertification in Mediterranean arid ecosystems. *Nature*, 449, 213–217.
- 589 Kitzberger, T., Aráoz, E., Gowda, J.H., Mermoz, M. & Morales, J.M. (2012). Decreases in Fire Spread Prob-
590 ability with Forest Age Promotes Alternative Community States, Reduced Resilience to Climate Variability
591 and Large Fire Regime Shifts. *Ecosystems*, 15, 97–112.
- 592 Koenker, R. (2016). quantreg: Quantile Regression.
- 593 Lasco, R.D., Pulhin, F.B., Cruz, R.V.O., Pulhin, J.M., Roy, S.S.N. & Sanchez, P.A.J. (2008). Forest
594 responses to changing rainfall in the Philippines. In: *Climate change and vulnerability* (eds. Leary, N.,
595 Conde, C. & Kulkarni, J.). Earthscan, London, pp. 49–66.
- 596 Leibold, M.A. & Norberg, J. (2004). Biodiversity in metacommunities: Plankton as complex adaptive
597 systems? *Limnology and Oceanography*, 49, 1278–1289.
- 598 Lenton, T.M. & Williams, H.T.P. (2013). On the origin of planetary-scale tipping points. *Trends in Ecology
599 & Evolution*, 28, 380–382.
- 600 Lenton, T.M., Held, H., Kriegler, E., Hall, J.W., Lucht, W. & Rahmstorf, S. *et al.* (2008). Tipping elements
601 in the Earth's climate system. *Proceedings of the National Academy of Sciences*, 105, 1786–1793.
- 602 Limpert, E., Stahel, W.A. & Abbt, M. (2001). Log-normal Distributions across the Sciences: Keys and
603 CluesOn the charms of statistics, and how mechanical models resembling gambling machines offer a link to
604 a handy way to characterize log-normal distributions, which can provide deeper insight into var. *BioScience*,
605 51, 341–352.
- 606 Loehle, C., Li, B.-L. & Sundell, R.C. (1996). Forest spread and phase transitions at forest-prairie ecotones
607 in Kansas, U.S.A. *Landscape Ecology*, 11, 225–235.
- 608 Malhi, Y., Gardner, T.A., Goldsmith, G.R., Silman, M.R. & Zelazowski, P. (2014). Tropical Forests in the

- 609 Anthropocene. *Annual Review of Environment and Resources*, 39, 125–159.
- 610 Manor, A. & Shnerb, N.M. (2008). Origin of pareto-like spatial distributions in ecosystems. *Physical Review*
611 *Letters*, 101, 268104.
- 612 McKenzie, D. & Kennedy, M.C. (2012). Power laws reveal phase transitions in landscape controls of fire
613 regimes. *Nat Commun*, 3, 726.
- 614 Mitchell, M.G.E., Suarez-Castro, A.F., Martinez-Harms, M., Maron, M., McAlpine, C. & Gaston, K.J. *et al.*
615 (2015). Reframing landscape fragmentation's effects on ecosystem services. *Trends in Ecology & Evolution*,
616 30, 190–198.
- 617 Naito, A.T. & Cairns, D.M. (2015). Patterns of shrub expansion in Alaskan arctic river corridors suggest
618 phase transition. *Ecology and Evolution*, 5, 87–101.
- 619 Newman, M.E.J. (2005). Power laws, Pareto distributions and Zipf's law. *Contemporary Physics*, 46, 323–
620 351.
- 621 Oborny, B., Meszéna, G. & Szabó, G. (2005). Dynamics of Populations on the Verge of Extinction. *Oikos*,
622 109, 291–296.
- 623 Oborny, B., Szabó, G. & Meszéna, G. (2007). Survival of species in patchy landscapes: percolation in space
624 and time. In: *Scaling biodiversity*. Cambridge University Press, pp. 409–440.
- 625 Ochoa-Quintero, J.M., Gardner, T.A., Rosa, I., de Barros Ferraz, S.F. & Sutherland, W.J. (2015). Thresholds
626 of species loss in Amazonian deforestation frontier landscapes. *Conservation Biology*, 29, 440–451.
- 627 Ódor, G. (2004). Universality classes in nonequilibrium lattice systems. *Reviews of Modern Physics*, 76,
628 663–724.
- 629 Pardini, R., Bueno, A. de A., Gardner, T.A., Prado, P.I. & Metzger, J.P. (2010). Beyond the Fragmentation
630 Threshold Hypothesis: Regime Shifts in Biodiversity Across Fragmented Landscapes. *PLoS ONE*, 5, e13666.
- 631 Potapov, P., Hansen, M.C., Stehman, S.V., Loveland, T.R. & Pittman, K. (2008a). Combining MODIS
632 and Landsat imagery to estimate and map boreal forest cover loss. *Remote Sensing of Environment*, 112,
633 3708–3719.
- 634 Potapov, P., Yaroshenko, A., Turubanova, S., Dubinin, M., Laestadius, L. & Thies, C. *et al.* (2008b).
635 Mapping the world's intact forest landscapes by remote sensing. *Ecology and Society*, 13.
- 636 Prishchepov, A.V., Müller, D., Dubinin, M., Baumann, M. & Radeloff, V.C. (2013). Determinants of

- 637 agricultural land abandonment in post-Soviet European Russia. *Land Use Policy*, 30, 873–884.
- 638 Pueyo, S., de Alencastro Graça, P.M.L., Barbosa, R.I., Cots, R., Cardona, E. & Fearnside, P.M. (2010).
639 Testing for criticality in ecosystem dynamics: the case of Amazonian rainforest and savanna fire. *Ecology
Letters*, 13, 793–802.
- 640
- 641 R Core Team. (2015). R: A Language and Environment for Statistical Computing.
- 642 Reyer, C.P.O., Rammig, A., Brouwers, N. & Langerwisch, F. (2015). Forest resilience, tipping points and
643 global change processes. *Journal of Ecology*, 103, 1–4.
- 644 Rooij, M.M.J.W. van, Nash, B., Rajaraman, S. & Holden, J.G. (2013). A Fractal Approach to Dynamic
645 Inference and Distribution Analysis. *Frontiers in Physiology*, 4.
- 646 Rudel, T.K., Coomes, O.T., Moran, E., Achard, F., Angelsen, A. & Xu, J. et al. (2005). Forest transitions:
647 towards a global understanding of land use change. *Global Environmental Change*, 15, 23–31.
- 648 Saravia, L.A. & Momo, F.R. (2017). Biodiversity collapse and early warning indicators in a spatial phase
649 transition between neutral and niche communities. *PeerJ PrePrints*, 5, e1589v4.
- 650 Scanlon, T.M., Caylor, K.K., Levin, S.A. & Rodriguez-iturbe, I. (2007). Positive feedbacks promote power-
651 law clustering of Kalahari vegetation. *Nature*, 449, 209–212.
- 652 Scheffer, M., Bascompte, J., Brock, W.A., Brovkin, V., Carpenter, S.R. & Dakos, V. et al. (2009). Early-
653 warning signals for critical transitions. *Nature*, 461, 53–59.
- 654 Scheffer, M., Walker, B., Carpenter, S., Foley, J. a, Folke, C. & Walker, B. (2001). Catastrophic shifts in
655 ecosystems. *Nature*, 413, 591–596.
- 656 Seidler, T.G. & Plotkin, J.B. (2006). Seed Dispersal and Spatial Pattern in Tropical Trees. *PLoS Biology*,
657 4, e344.
- 658 Sexton, J.O., Noojipady, P., Song, X.-P., Feng, M., Song, D.-X. & Kim, D.-H. et al. (2015). Conservation
659 policy and the measurement of forests. *Nature Climate Change*, 6, 192–196.
- 660 Sexton, J.O., Song, X.-P., Feng, M., Noojipady, P., Anand, A. & Huang, C. et al. (2013). Global, 30-m
661 resolution continuous fields of tree cover: Landsat-based rescaling of MODIS vegetation continuous fields
662 with lidar-based estimates of error. *International Journal of Digital Earth*, 6, 427–448.
- 663 Solé, R.V. (2011). *Phase Transitions*. Primers in complex systems. Princeton University Press.
- 664 Solé, R.V. & Bascompte, J. (2006). *Self-organization in complex ecosystems*. Princeton University Press,

- 665 New Jersey, USA.
- 666 Solé, R.V., Alonso, D. & Mckane, A. (2002). Self-organized instability in complex ecosystems. *Philosophical*
667 *transactions of the Royal Society of London. Series B, Biological sciences*, 357, 667–681.
- 668 Solé, R.V., Alonso, D. & Saldaña, J. (2004). Habitat fragmentation and biodiversity collapse in neutral
669 communities. *Ecological Complexity*, 1, 65–75.
- 670 Solé, R.V., Bartumeus, F. & Gamarra, J.G.P. (2005). Gap percolation in rainforests. *Oikos*, 110, 177–185.
- 671 Staal, A., Dekker, S.C., Xu, C. & Nes, E.H. van. (2016). Bistability, Spatial Interaction, and the Distribution
672 of Tropical Forests and Savannas. *Ecosystems*, 19, 1080–1091.
- 673 Stauffer, D. & Aharony, A. (1994). *Introduction To Percolation Theory*. Taylor & Francis, London.
- 674 Taubert, F., Fischer, R., Groeneveld, J., Lehmann, S., Müller, M.S. & Rödig, E. et al. (2018). Global
675 patterns of tropical forest fragmentation. *Nature*.
- 676 Vasilakopoulos, P. & Marshall, C.T. (2015). Resilience and tipping points of an exploited fish population
677 over six decades. *Global Change Biology*, 21, 1834–1847.
- 678 Villa Martín, P., Bonachela, J.A. & Muñoz, M.A. (2014). Quenched disorder forbids discontinuous transitions
679 in nonequilibrium low-dimensional systems. *Physical Review E*, 89, 12145.
- 680 Villa Martín, P., Bonachela, J.A., Levin, S.A. & Muñoz, M.A. (2015). Eluding catastrophic shifts. *Proceed-
681 ings of the National Academy of Sciences*, 112, E1828–E1836.
- 682 Viña, A., McConnell, W.J., Yang, H., Xu, Z. & Liu, J. (2016). Effects of conservation policy on China's
683 forest recovery. *Science Advances*, 2, e1500965.
- 684 Vuong, Q.H. (1989). Likelihood Ratio Tests for Model Selection and Non-Nested Hypotheses. *Econometrica*,
685 57, 307–333.
- 686 Weerman, E.J., Van Belzen, J., Rietkerk, M., Temmerman, S., Kéfi, S. & Herman, P.M.J. et al. (2012).
687 Changes in diatom patch-size distribution and degradation in a spatially self-organized intertidal mudflat
688 ecosystem. *Ecology*, 93, 608–618.
- 689 Weissmann, H. & Shnerb, N.M. (2016). Predicting catastrophic shifts. *Journal of Theoretical Biology*, 397,
690 128–134.
- 691 Wuyts, B., Champneys, A.R. & House, J.I. (2017). Amazonian forest-savanna bistability and human impact.

- 692 *Nature Communications*, 8, 15519.
- 693 Xu, C., Hantson, S., Holmgren, M., Nes, E.H. van, Staal, A. & Scheffer, M. (2016). Remotely sensed canopy
- 694 height reveals three pantropical ecosystem states. *Ecology*, 97, 2518–2521.
- 695 Zhang, J.Y., Wang, Y., Zhao, X., Xie, G. & Zhang, T. (2005). Grassland recovery by protection from grazing
- 696 in a semi-arid sandy region of northern China. *New Zealand Journal of Agricultural Research*, 48, 277–284.
- 697 Zinck, R.D. & Grimm, V. (2009). Unifying wildfire models from ecology and statistical physics. *The*
- 698 *American naturalist*, 174, E170–85.